Current Research in Food Science 9 (2024) 100805

Contents lists available at ScienceDirect

Current Research in Food Science

journal homepage: www.sciencedirect.com/journal/current-research-in-food-science

Konjac supplementation can alleviate obesity induced by high-fat diet in mice by modulating gut microbiota and its metabolites

Yuhang Wen [a,b,c,1], Baoting Chen [a,b,c,1], Jingrong Huang [a,b,c,1], Yadan Luo [a,b,c], Shuya Lv [a,b,c], Hao Qiu [a,b,c], Shuaibing Li [a,b,c,e], Songwei Liu [a,b,c], Lvqin He [a,b,c], Manli He [a,b,c], Zehui Yu [a,b,c], Mingde Zhao [a,b,c], Qian Yang [a,b,c,**], Dong Li [d,***], Congwei Gu [a,b,c,*]

[a] Laboratory Animal Centre, Southwest Medical University, Luzhou, China
[b] Model Animal and Human Disease Research of Luzhou Key Laboratory, Southwest Medical University, Luzhou, China
[c] Department of Nutrition and Food Hygiene, School of Public Health, Southwest Medical University, Luzhou, China
[d] College of Bioengineering, Sichuan University of Science and Engineering, Yibin, 643002, China
[e] School of Traditional Chinese Medicine, Shenyang Pharmaceutical University, Shenyang, 110016, China

ARTICLE INFO

Handling editor: Yeonhwa Park

Keywords:
Konjac supplementation
16S rDNA sequencing
Untargeted metabolomics
Association analysis
High-fat diet
Obesity

ABSTRACT

As a multi-factorial disease, obesity has become one of the major health problems in the world, and it is still increasing rapidly. Konjac supplementation, as a convenient dietary therapy, has been shown to be able to regulate gut microbiota and improve obesity. However, the specific mechanism by which konjac improves obesity through gut microbiota remains to be studied. In this study, a high-fat diet (HFD) was used to induce a mouse obesity model, and 16S rDNA sequencing and an untargeted metabolomics were used to investigate the impact of konjac on gut microbiota and gut metabolites in HFD-induced obese mice. The results show that konjac can reduce the body weight, adipose tissue weight, and lipid level of high-fat diet induced obese mice by changing the gut microbiota structure and gut metabolic profile. Association analysis revealed that konjac supplementation induced changes in gut microbiota, resulting in the up-regulation of 7-dehydrocholesterol and trehalose 6-phosphate, as well as the down-regulation of glycocholic acid and ursocholic acid within the Secondary bile acid biosynthesis pathway, ultimately leading to improvements in obesity. Among them, *g_Acinetobacter* (Greengene ID: 911888) can promote the synthesis of 7-dehydrocholesterol by synthesizing ERG3. *g_Allobaculum* (Greengene ID: 271516) and *g_Allobaculum* (Greengene ID: 259370) can promote the breakdown of trehalose 6-phosphate by synthesizing glvA. Additionally, the down-regulation of glycocholic acid and ursocholic acid may be influenced by the up-regulation of *Lachnospiraceae_NK4A136_group*. In conclusion, konjac exerts an influence on gut metabolites through the regulation of gut microbiota, thereby playing a pivotal role in alleviating obesity induced by a high-fat diet.

1. Introduction

Over two billion people worldwide suffer from obesity, a condition characterized by abnormal accumulation of white adipose tissue (Caballero, 2019; Chandrasekaran and Weiskirchen, 2024). Furthermore, obesity is a significant public health concern because of its association with diabetes, cardiovascular disease, and cancer (Caruso et al., 2023). The pathogenesis and progression of obesity, as well as its impacts on human health, have been largely elucidated by global scientific researchers over the past few years (Aron-Wisnewsky et al., 2019; Breit et al., 2023; Marcelin et al., 2019). Despite these advances, the complex etiology and multiorgan damage associated with obesity present challenges in developing a practical and efficient treatment. Therefore, it is imperative to conduct additional research on the causes and

* Corresponding author.
** Corresponding author.
*** Corresponding author.
E-mail addresses: yangqiansicau@126.com (Q. Yang), 4469344@qq.com (D. Li), gcw081543@swmu.edu.cn (C. Gu).
[1] Authors contributed equally to the study.

https://doi.org/10.1016/j.crfs.2024.100805
Received 24 April 2024; Received in revised form 17 June 2024; Accepted 8 July 2024
Available online 14 July 2024

advancement of obesity, as well as to devise straightforward and efficient treatment and intervention approaches. This will not only improve the well-being of individuals and overall health outcomes but also reduce the financial strain on healthcare systems.

Dietary therapy and traditional medicine are viable approaches to tackling obesity, with konjac powder emerging as a popular option owing to its natural health benefits. The primary component of konjac powder, konjac glucomannan (KGM), not only enhances the taste of food and keeps it fresh, but also regulates blood sugar, blood lipids, gut microbiota, oxidative stress, and immune function (Ho et al., 2017; Jian et al., 2017; Rogovik and Goldman, 2009; Zhao et al., 2020). Concurrently, KGM demonstrates the capacity to extend gastric emptying, enhance satiety, stimulate liver glycogen synthesis, enhance gut microbiota and metabolic functions via diverse molecular pathways, consequently influencing oxidative stress and immune inflammation regulation, and providing hepatoprotective and nephroprotective effects (Tester and Al-Ghazzewi, 2016). However, the specific mechanism by which konjac exerts the bioactive role of anti-obesity is still controversial. While Xu et al. demonstrated that konjac may reduce obesity by increasing satiety and decreasing energy consumption (C. Xu et al., 2023), conflicting results were reported by Hong et al. and Liu et al. who found that konjac supplementation did not lead to a reduction in energy intake (Hong et al., 2023; Liu et al., 2023). As a result, further investigation into the mechanisms behind konjac's beneficial effects is warranted to improve our understanding of obesity treatment.

The gut microbiota is recognized as a significant contributor to the pathogenesis of metabolic disorders and functions as an endocrine organ that plays a role in regulating energy balance and immune responses (Marchesi et al., 2016). The dysregulation of gut microbiota is a prominent characteristic of obesity, characterized by noticeable differences in microbial diversity between individuals with obesity and those without. This disturbance in the gut ecosystem can compromise the integrity of the gut barrier, causing changes in the levels of various gut metabolites including short-chain fatty acids (SCFAs), indole derivatives, and polyamines. These alterations have the potential to disrupt lipid metabolism and initiate inflammatory processes, ultimately contributing to the development of obesity (Boulangé et al., 2016; Cani et al., 2009; Cuevas-Sierra et al., 2019). Mechanistic investigations have demonstrated that oral KGM supplementation enhances the growth of beneficial gut microbiota, modulates the gut microenvironment, and attenuates inflammation (Jiang et al., 2018). These results highlight the substantial role of gut microbiota in mediating the beneficial effects of konjac on obesity. However, additional studies are necessary to explore the effects of konjac powder supplementation on the metabolic interactions between gut microbiota and its metabolites in the context of a high-fat diet.

The aim of the study is to investigate what impact konjac powder might have on the gut microbiota and gut metabolites of mice who have been induced to become obese by high-fat diets. Utilizing 16S rDNA sequencing and non-targeted metabolomics, the relationship between konjac, gut microbiota, and gut metabolites was examined to elucidate the potential mechanism by which konjac may alleviate obesity.

2. Materials and methods

2.1. The preparation of konjac powder

A white konjac (from Pingshan County, Yibin City, Sichuan Province, China) was cut into pieces and dried. It was then crushed by a portable grinder at room temperature and ground by a planetary ball mill. In 2 h, 200 rpm was used to grind the konjac, resulting in crude powder. Konjac glucomannan (KGM) was subsequently purified from crude konjac powder through a process involving dissolution of 60% alcohol and crude konjac powder at a volume ratio of 100:1, sonication for 20 min, microwave heating at 350 W for 20 s, vacuum filtration, and drying to yield konjac powder. The purified konjac powder contains a high concentration of KGM, exceeding 85% (Dong Li et al., 2020). A solution of konjac powder was prepared by adding it to saline at a concentration of 0.08 g/ml for use in subsequent experiments involving mice.

2.2. Animal feeding and sample collection

Six-week-old male C57BL/6J mice, bred under specific pathogen-free (SPF) conditions, were obtained from Beijing Vital River Laboratory Animal Technology Co., Ltd. The mice were housed in the SPF barrier system of the Experimental Animal Center of Southwest Medical University, maintained at an ambient temperature of 22 ± 2 °C, humidity of 50%–60%, and a 12-h light-dark cycle. Throughout the experiment, the mice had ad libitum access to food and water. Following a one-week acclimation period, the C57BL/6 J mice were randomly assigned to either a control (CK) group or a high-fat diet (HFD) group. The high-fat diet (D12492) supplied by Research Diets is composed of 20% of calories derived from carbohydrates, 20% from protein, and 60% from fat. Detailed ingredients of the normal diet and the HFD can be found in Supplement table 1. At the twelfth week of the study, mice that had been fed a high-fat diet were randomly assigned to either the model control (MK) group (n = 6) or the konjac (KON) group (n = 6), while mice on the control diet (CK) (n = 6) maintained their original diet. The KON group received a daily dose of konjac powder (0.8 g/kg) in addition to their high-fat diet for a duration of 5 weeks, as well as 0.1 ml of the konjac solution per 10 g of body weight via gavage. In contrast, CK and MK mice received an equivalent volume of normal saline daily via gavage, in addition to their regular diet. The konjac powder utilized in the study was supplied by Sichuan University of Science & Engineering. Following the completion of the experiment, all mice underwent an overnight fast and were anesthetized with 1% pentobarbital sodium (50 mg/kg) in the early morning of the subsequent day prior to euthanasia by cervical dislocation. Blood samples were promptly obtained and allowed to acclimate to room temperature. Adipose tissue surrounding the testis was harvested and weighed. The cecal contents situated distal to the ileocecal valve were collected and preserved at −80 °C for subsequent analysis using 16S rDNA sequencing and untargeted metabolome profiling.

2.3. Pathological section of adipose tissue

Adipose tissue surrounding the epididymis was preserved in 4% paraformaldehyde, washed, dehydrated, embedded in paraffin, sectioned into 4 μm slices, and subsequently stained with hematoxylin-eosin (H&E). Photographs of the sample tissue were taken under a microscope for assessing adipose tissue histopathological features, and Image Pro Plus 6.0 was used for measuring and analyzing adipose cell area.

2.4. Serum biochemical analysis

The collected blood samples were left at room temperature for 4 h, centrifuged at 4 °C and 3500r/min for 10 min, then the serum was collected. An equivalent volume of serum was extracted from each sample, and the concentrations of triglycerides (TG), total cholesterol (TC), low-density lipoprotein (LDL), and high-density lipoprotein (HDL) in the serum were measured using the TC220 automatic veterinary biochemical analyzer (manufactured by Tekang Technology Co., Ltd.).

2.5. 16S rDNA sequencing

The genomic DNA of gut microbiota in cecum contents was extracted using HiPure Stool DNA Kit (D3141, Guangzhou Meiji Biological Co., LTD., China). 16S rDNA V3–V4 region was amplified using a specific primer (341F, CCTACGGGRBGCASCAG; 806R: GGACTACNNGGGTATCTAAT). Subsequently, the amplified products were quantified, purified, and utilized for library construction and sequencing. Following the sequencing process, raw reads were obtained and subsequently

filtered for low quality using FASTP (V0.18.0, https://github.com/OpenGene/fastp). Afterward, FLASH (V1.2.11, http://www.cbcb.umd.edu/software/flash) was employed to splice reads to obtain tags. The tags acquired were subsequently subjected to filtration and elimination of chimeras to procure efficient tags. Abundance statistics for Operational Taxonomic Units (OTUs) were subsequently computed utilizing the filtered tags. After comparing the sequence information of the OTUs with the SILVA database, species annotation information for each OTU was obtained. Linear discriminant analysis effect size (LEfSe) analysis (V1.0, http://huttenhower.sph.harvard.edu/lefse/) was used to detect biomarkers in gut microbiota, and species with LDA value > 4 were selected as biomarkers. Alpha diversity analysis was performed using QIIME (V1.9.1, http://qiime.sourceforge.net/). R studio was used to conduct beta diversity analysis, including PCoA and NMDS analyses based on linear and nonlinear models.

2.6. Untargeted metabolomics

The cecal contents were thawed at 4 °C and subsequently mixed with a solution consisting of methanol, acetonitrile, and water in a 2:2:1 ratio (v/v). The mixture was then subjected to ultrasound treatment at low temperature for 30 min, followed by incubation at −20 °C for 10 min. Subsequently, the supernatant was obtained by centrifugation at 14000*g* for 20 min at 4 °C. An equal volume was taken from each sample to be tested and mixed together as a quality control (QC) sample. Sample supernatant was placed into the Liquid Chromatograph-Mass Spectrometer (LC-MS) for analysis. Ultra-High performance liquid chromatography (UHPLC, Agilent 1290 Infinity LC) HILIC column was used for separation: column temperature 25 °C; flow rate 0.5 ml/min; sample size 2 μL; mobile phase A: water +25 mM ammonium acetate +25 mM ammonia water; and mobile phase B: acetonitrile. Random sequential sampling was employed to assess the stability of the system. Subsequently, the primary and secondary spectra of the samples were acquired using the AB Sciex TripleTOF 6600 mass spectrometer after elution (Shanghai Applied Protein Technology Co., Ltd.). The ESI source parameters were configured as follows: Ion Source Gas1 (Gas1) set to 60, Ion Source Gas2 (Gas2) set to 60, curtain gas (CUR) set to 30, source temperature set to 600 cquired using the AB Sciex TripleTOF 6600 mass spectrome During MS acquisition, the instrument was configured to capture mass-to-charge ratios ranging from 60 to 1000 Da, with an accumulation time of 0.20 s per spectra for the TOF MS scan. The production scan was performed utilizing information dependent acquisition (IDA) in high sensitivity mode, with specific parameters set as follows: a fixed collision energy (CE) of 35 V with a range of ±15 eV; declustering potential (DP) of 60 V (+) and −60 V (−); exclusion of isotopes within 4 Da, and monitoring of 10 candidate ions per cycle. Following this, the molecular characteristic peaks in secondary mass spectrometry were identified, and substance annotations were conducted in conjunction with Mass Bank, Metlin, MoNA, and other publicly available databases. Multivariate statistical analysis and cluster analysis were executed using R studio. Additionally, pathway enrichment analysis was performed utilizing the Kyoto Encyclopedia of Genes and Genomes (KEGG) database.

2.7. MIMOSA2 analysis

MIMOSA2 analysis (http://elbo-spice.cs.tau.ac.il/shiny/MIMOSA2shiny/) (Noecker et al., 2022) involves a regression analysis that utilizes a database to forecast microbial metabolic potential and subsequently establishes correlations between the predicted metabolic potential and observed metabolomic data. Following the annotation of OTU sequences in various databases such as KEGG, NCBI, EMBL-EBI, VMH, and others, MIMOSA2 developed a network prediction model of metabolic capacity utilizing OTU abundance and established metabolic functions. This model was employed to compute the Metabolic Potential (MP) score for each microbial taxon, facilitating the prediction of the influence of individual microbial units on metabolites present in the sample. Furthermore, a Community-level Metabolic Potential (CMP) score was generated by consolidating the metabolic potentials of all microbial units.Subsequently, the CMP scores were subjected to regression analysis against metabolite abundances determined through metabolomics, employing a rank prediction-based regression model to evaluate the predictive capability of CMP scores on metabolite levels. If $P < 0.1$, it was considered that the change in metabolite level was mediated by microorganisms. Finally, the overall model fit was decomposed into the contribution from each taxon, and the specific taxa that can explain variation in each metabolite was identified.

2.8. Statistical analysis

This study used SPSS 25.0 statistical analysis software for data statistical analysis. The *Shapiro-Wilk test* was used to perform a normal test on the data, *one-way ANOVA* was performed on the data conforming to normal distribution. Among them, those with homogeneous variance were analyzed by *Bonferroni*, and those with heterogeneous variance were analyzed using by *Tamhane's T2*. The *Kruskal-Wallis rank sum test* was performed on the data not conforming to normal distribution. All values were expressed using mean ± SD. Spearman statistical analysis was used to analyze the correlation between different types of data in the sample, and R studio was used for matrix thermal mapping and hierarchical clustering. $P < 0.05$ shows that the experimental results in statistical significant difference, $P < 0.01$ shows that the result of the experiment is extremely remarkable difference in statistics.

3. Results

3.1. The effect of konjac on the phenotype of obese mice

After 12 weeks of HFD, the body weight of HFD mice was significantly higher than that of CK mice (Fig. 1A, $P < 0.05$). Before Konjac supplementation, there was no significant difference in body weight between KON and MK mice (Fig. 1B). After konjac supplementation, KON mice continued to lose body weight, with a significant difference from MK mice at week 13 ($P < 0.05$), and the significant difference from CK mice disappeared at week 16 (Fig. 1B). There was no significant difference in total food intake and energy intake between KON and MK mice over the course of the 5-week konjac supplementation period (Supplement Figs. 1a–b). In addition, the adipose tissue weight and the percentage of adipose tissue weight to body weight of MK mice were significantly higher than that of CK mice after HFD ($P < 0.01$), but after konjac supplementation, the adipose tissue weight as well as the percentage of adipose tissue weight to body weight of KON mice were significantly lower than that of MK group (Fig. 1C–D, $P < 0.05$). From the H&E staining, we observed that konjac supplementation also had the effect of reducing the area of adipocytes (Fig. 1E), but after calculating the average area of adipocytes in the sections, we found that this effect was not significant (Fig. 1F). After HFD, the serum levels of TC, LDL, and HDL in MK mice were significantly higher than those in CK mice (Fig. 1G, $P < 0.01$). After konjac supplementation, serum TC, TG, and HDL levels in KON mice were significantly lower than those in MK mice (Fig. 1G, $P < 0.05$). These results suggest that konjac glucomannan (KGM) in konjac powder could significantly reduce the HFD-induced increase in body weight, adipose tissue weight, and serum lipid levels in mice.

3.2. The effects of konjac on gut microbiota in obese mice

3.2.1. Alpha diversity and beta diversity

The Alpha diversity analysis revealed that the ACE, Chao1, and Shannon indices of gut microbiota in CK mice were significantly higher compared to those in MK and KON mice ($P < 0.05$). However, there was no significant difference observed between MK and KON mice in this

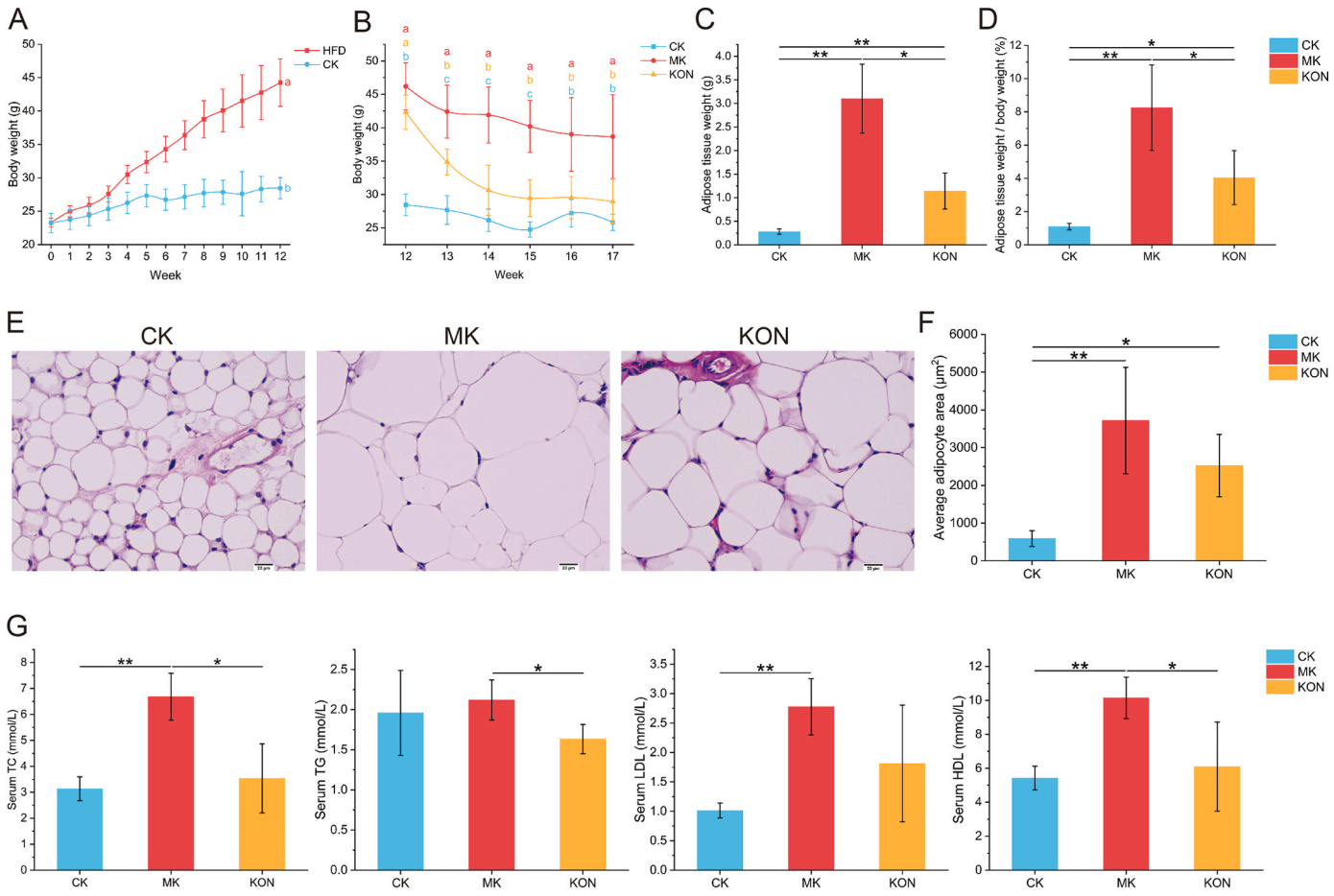

Fig. 1. Konjac supplementation can significantly reduce the increase of body weight, adipose tissue weight, and serum lipid level induced by HFD in mice (n = 6 per group). (A) Body weight of mice in the high-fat diet induced obesity model (0–12 weeks); (B) body weight of mice during konjac supplementation (12–17 weeks); (C) adipose tissue weight; (D) the percentage of adipose tissue weight to body weight; (E) H&E stained pathological sections of adipose tissue (× 400); (F) average adipocyte area; and (G) serum TC, TG, LDL and HDL levels. Different lowercase letters indicate significant differences between groups. "*" indicates $P < 0.05$ and "**" indicates $P < 0.01$.

regard (Fig. 2A). The Simpson index also did not differ significantly among the three groups of mice (Fig. 2A). This indicates that konjac supplementation did not significantly alter the Alpha diversity of the gut microbiota. However, in the Beta diversity analysis, PCoA analysis and NMDS analysis both showed a clear separation trend between gut microbiota of CK, MK, and KON mice (Fig. 2B). The stress value in NMDS analysis was less than 0.2, indicating that the model could accurately reflect the differences between samples. These results indicate that KGM in konjac powder can significantly affect the gut microbiota structure of HFD-induced mice.

3.2.2. *LEfSe analysis*

We screened the biomarkers of genus level in each group. The biomarkers in CK mice were *Marvinbryantia*, *Candidatus_Saccharimonas*, and *Allobaculum*. The biomarkers of MK mice were *Coriobacteriaceae_UCG_002*, *Colidextribacter*, *Faecalibaculum*, *Blautia*, and *Dubosiella*. The biomarker in KON mice was *Lachnospiraceae_NK4A136_group* (Fig. 2C–D).

3.2.3. *Species composition analysis of gut microbiota*

Venn diagrams show that the three groups of mice shared 283 OTUs, accounting for 22% of the total OTUs. The number of OTUs unique to CK, MK, and KON mice was 505, 136, and 175, respectively, accounting for 39%, 10%, and 13% of the total OTUs, respectively (Fig. 2E). Stacked plots show the top 10 phyla level bacteria by relative abundance, among which *Bacteroidota* was significantly downregulated in both MK and KON mice relative to CK mice, and *Desulfobacterota* and *Patescibacteria* were significantly up-regulated and down-regulated in KON mice compared with CK mice, respectively (Fig. 2F, $P < 0.05$). In addition, *Actinobacteriota* was down-regulated in KON mice relative to MK mice after konjac supplementation (Fig. 2F, $P < 0.05$). At the genus level, it is noteworthy that eight of the top 20 genera in relative abundance were biomarkers in the LEfSe analysis (Fig. 2G). Among them, the relative abundance of MK mice biomarkers *Coriobacteriaceae_UCG_002*, *Colidextribacter*, *Faecalibaculum*, *Blautia*, and *Dubosiella* was significantly up-regulated in MK mice compared with CK mice ($P < 0.05$). *Lachnospiraceae_NK4A136_group*, a biomarker in KON mice, was significantly up-regulated as compared to MK mice ($P < 0.05$). Biomarkers of CK mice, *Candidatus_Saccharimonas* and *Allobaculum*, were both significantly up-regulated in CK mice relative to MK and KON mice (Fig. 2G, $P < 0.05$).

3.3. *The effects of konjac on gut metabolites in obese mice*

3.3.1. *Multivariate statistical analysis and screening of differential metabolites*

PCA, PLS-DA and OPLS-DA all show a significant trend of separation between gut metabolites in both positive and negative ion modes in the three groups of mice (Supplement Figs. 2a–c). The R2Y values in PLS-DA and OPLS-DA were greater than 0.7, and the permutation test based on OPLS-DA show that the intersection point of Q2 regression curve and ordinate of all models was less than 0 (Supplement Fig. 2d). This

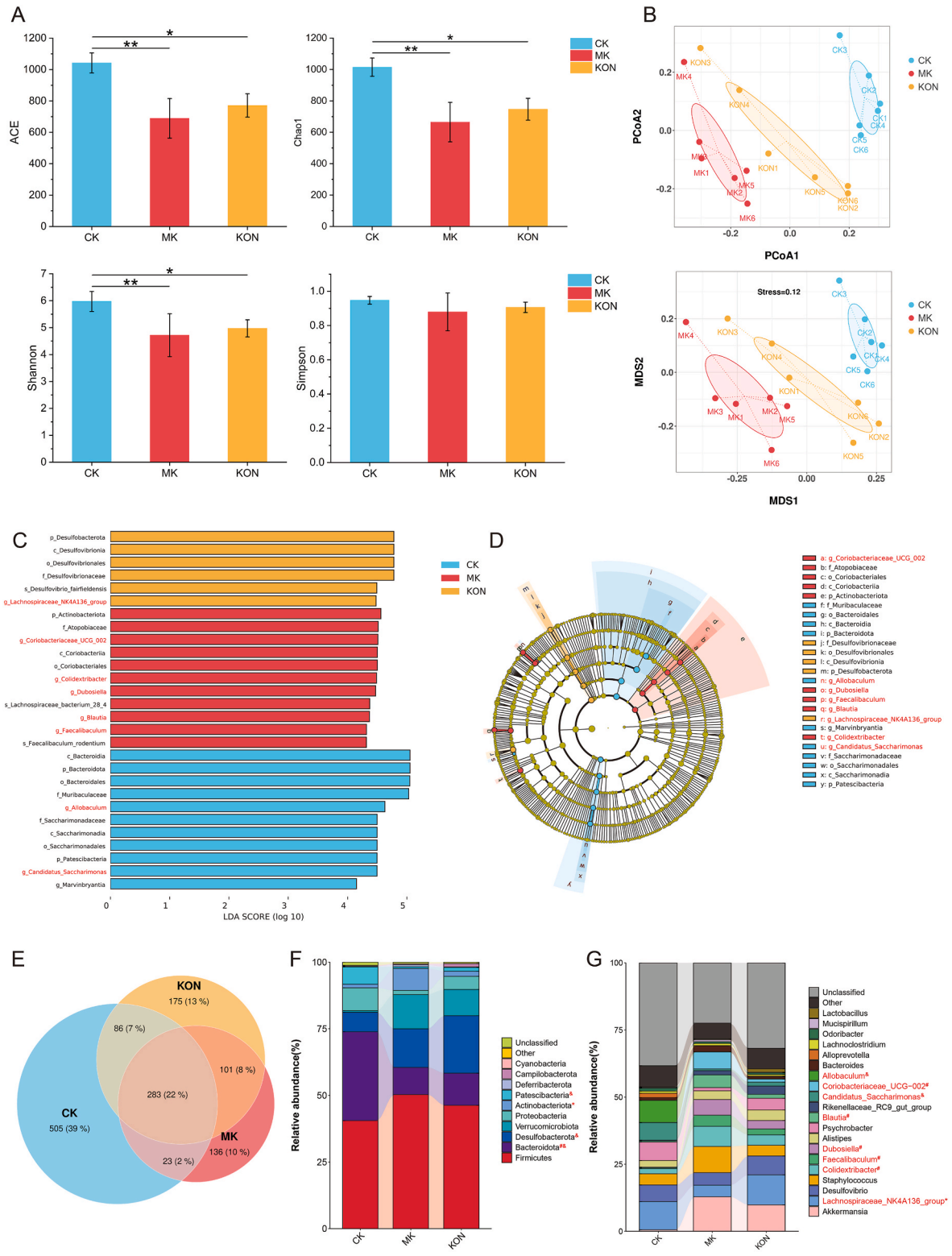

Fig. 2. Konjac supplementation significantly alters the structure and species composition of gut microbiota in mice after HFD (n = 6 per group). (A) Alpha diversity analysis, including ACE, Chao1, Shannon, and Simpson values; (B) beta diversity analysis, including PCoA and NMDS analysis; (C) Score diagram and (D) evolutionary branching diagram of bacteria with LDA score greater than 4 in LEfSe analysis; (E) venn diagram of the number of OTUs in each group; (F) phyla level bacteria with the top 10 relative abundances; and (G) genera level bacteria with the top 20 relative abundance. "#" indicates a significant difference between CK and MK mice, "&" indicates a significant difference between CK and KON mice, and "*" indicates a significant difference between MK and KON mice, $P < 0.05$.

indicates that the model predictions are reliable and that no overfitting occurred. Metabolites with VIP >1 and P < 0.05 were classified as differential metabolites. A total of 2778 differential metabolites were detected across the three groups. Specifically, 970 metabolites were found to be significantly up-regulated and 982 metabolites were significantly down-regulated in MK mice, while 944 metabolites were significantly up-regulated and 828 metabolites were significantly down-regulated in KON mice compared to CK mice (Supplement Fig. 2e, $P < 0.05$). A statistical analysis revealed that 515 metabolites exhibited significant up-regulation, while 395 metabolites exhibited significant down-regulation in KON mice compared to MK mice (Supplement Fig. 2e, $P < 0.05$).The cluster heatmap shows the distribution of these differential metabolites (Fig. 3A). Among them, 7-dehydrocholesterol and trehalose 6-phosphate were up-regulated after HFD, while glycocholic acid and ursocholic acid were down-regulated (Fig. 3A).

3.3.2. KEGG pathway enrichment analysis and obesity-related differential metabolites

The KEGG pathway enrichment analysis was performed to explore the changes in metabolic pathways. The results show that the differential metabolites between CK and MK mice and between CK and KON mice were significantly enriched in Steroid hormone biosynthesis, Steroid biosynthesis, Primary bile acid biosynthesis, Phenylalanine metabolism, and ABC transporters (Fig. 3B–C, $P < 0.05$). In addition, the differential metabolites between KON and MK mice were significantly enriched in Secondary bile acid biosynthesis, Starch and sucrose metabolism, HMG-CoA reductase inhibitors and Vitamin B6 metabolism (Fig. 3D, $P < 0.05$). Meanwhile, the differential metabolites between KON and CK mice were also significantly enriched in Secondary bile acid biosynthesis (Fig. 3C, $P < 0.05$). Notably, two differential metabolites enriched in the Secondary bile acid biosynthesis pathway, glycocholic acid and ursocholic acid, are both widely believed to be positively associated with the development of obesity. In our study, both glycocholic acid and ursocholic acid were significantly upregulated in MK mice, but this was significantly reversed by konjac supplementation (Fig. 3E, $P < 0.01$). Trehalose 6-phosphate and trehalose, which were enriched in Starch and sucrose metabolism pathways, are both thought to be negatively correlated with obesity, and they were both significantly up-regulated after konjac supplementation (Fig. 3F, $P < 0.05$). In addition, when other differential metabolites were analyzed, we found that 7-dehydrocholesterol, which has the effect of alleviating obesity, was significantly down-regulated in MK mice, while konjac supplementation significantly up-regulated their levels in KON mice relative to MK mice (Fig. 3G, $P < 0.01$).

3.4. Association analysis between gut 16S rDNA sequencing and untargeted metabolome

3.4.1. Correlation analysis between gut microbiota and differential metabolites

To investigate the effect of konjac on gut metabolites through gut microbiota, a correlation analysis was done on eight biomarkers from the top 20 genera in relative abundance and differential metabolites in four KEGG metabolic pathways that were significantly enriched in KON mice compared to MK mice. The results show that both glycocholic acid and ursocholic acid in Secondary bile acid biosynthesis were significantly positively correlated with the biomarkers of MK mice, *Coriobacteriaceae_UCG_002*, *Faecalibaculum*, *Blautia*, and *Dubosiella* (Fig. 4A, $P < 0.05$). Glycocholic acid and ursocholic acid were also significantly negatively correlated with the biomarkers of CK and KON mice,

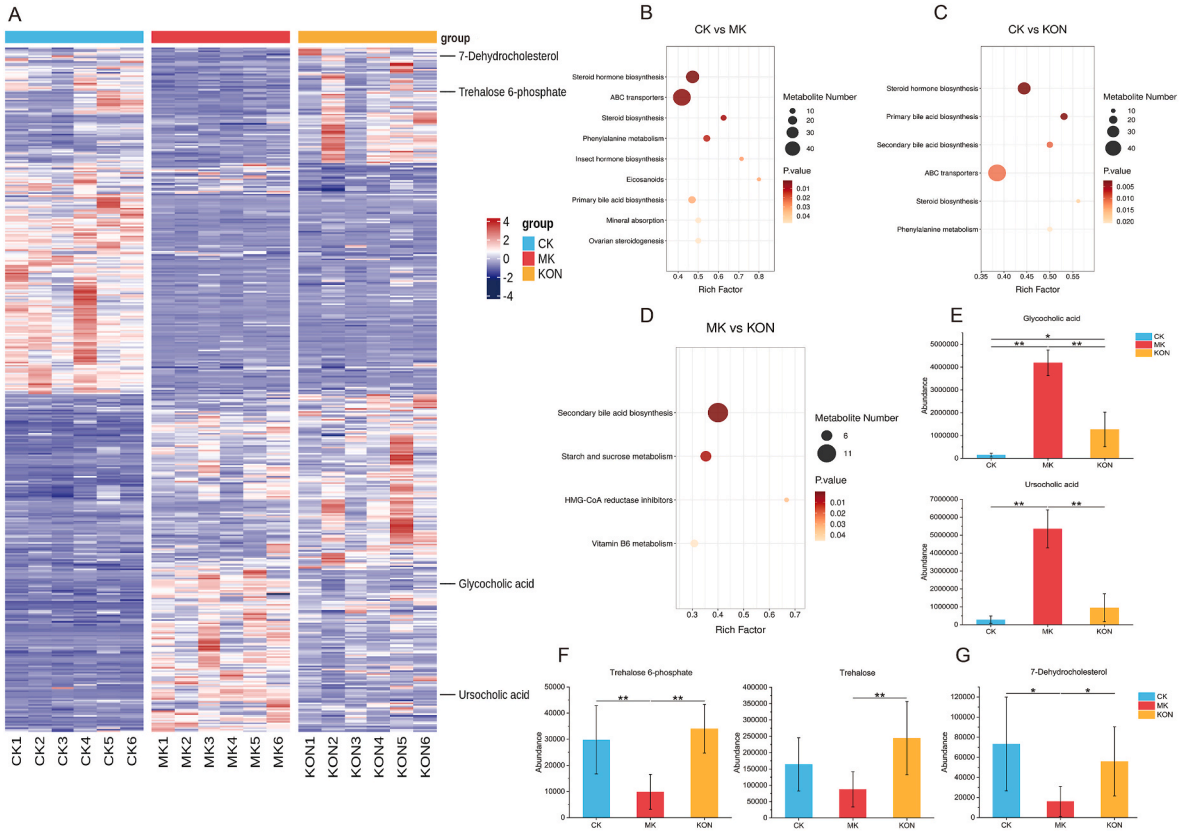

Fig. 3. Konjac supplementation can significantly change the gut metabolites of mice after HFD (n = 6 per group). (A) Differential metabolite cluster heat map; (B) KEGG pathway enrichment bubble map of CK vs MK; (C) KEGG pathway enrichment bubble map of CK vs KON; (D) KEGG pathway enrichment bubble map of MK vs KON; (E) abundance of glycocholic acid and ursocholic acid; (F) abundance of trehalose 6-phosphate and trehalose; and (G) abundance of 7-dehydrocholesterol. "*" indicates $P < 0.05$ and "**" indicates $P < 0.01$.

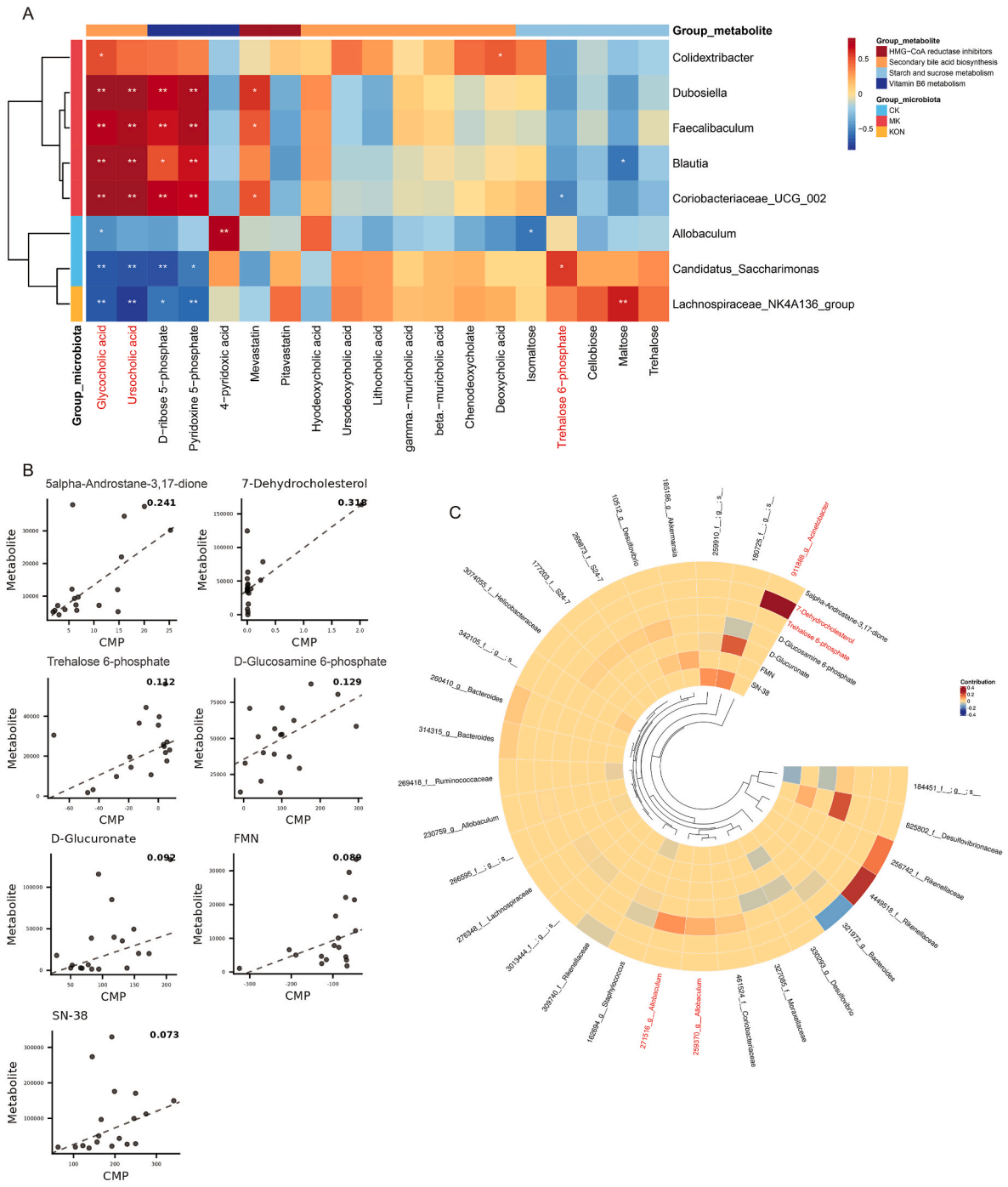

Fig. 4. Analysis of the correlation between gut microbiota and differential metabolites (n = 6 per group). (A) Heat map of correlation analysis of differential metabolites and biomarkers in LEfSe analyses; (B) regression scatter plots of CMP values and actual abundances of seven metabolites regulated by gut microbiota in MIMOSA2 analysis; and (C) heat map of the contribution of each gut microbiota taxon to alterations in these seven metabolites. "*" indicates $P < 0.05$ and "**" indicates $P < 0.01$.

Candidatus_Saccharimonas and *Lachnospiraceae_NK4A136_group* (Fig. 4A, $P < 0.05$). In addition, trehalose 6-phosphate was significantly negatively correlated with *Coriobacteriaceae_UCG_002*, a biomarker of MK mice, and positively correlated with *Candidatus_Saccharimonas*, a biomarker of CK mice (Fig. 4A, $P < 0.05$).

3.4.2. MIMOSA2 analysis

To further explore the specific role of gut microbiota on gut metabolites, we performed a MIMOSA2 analysis. The results show that there were seven differential metabolites with significant regression relationships between CMP values and the actual detected abundance in the metabolome, including 5alpha-androstane-3,17-dione, 7-dehydrocholesterol, trehalose 6-phosphate, D-glucosamine 6-phosphate, D-glucuronate, FMN, and SN-38 (Fig. 4B, $P < 0.1$). This suggests that the gut microbiota mediated the changes in these seven metabolites. Subsequently, we identified the key contributors in the gut microbiota responsible for these metabolite changes. Among them, *g_Acinetobacter* (Greengene ID: 911888) can mediate the synthesis of 7-dehydrocholesterol by synthesizing delta7-sterol 5-desaturase (ERG3, K00227). It also had a positive contribution to the change in the level of 7-

dehydrocholesterol (Fig. 4C). In addition, *g_Allobaculum* (Greengene ID: 271516) and *g_Allobaculum* (Greengene ID: 259370) can mediate the decomposition of trehalose 6-phosphate by synthesizing maltose 6′-phosphate glucosidase (glvA, K01232). Both had a positive contribution to the change in the level of trehalose 6-phosphate (Fig. 4C). This suggests that both the downregulation of 7-dehydrocholesterol and trehalose 6-phosphate in MK mice and the upregulation in KON mice were mediated by the gut microbiota.

3.4.3. Correlation analysis between gut microbiota, differential metabolites, and obesity-related phenotypes

In order to delve deeper into the connection between the markedly changed gut microbiota, gut metabolites, and obesity-related phenotypes, the biomarkers within the top 20 genera and obesity-related differential metabolites were analyzed in relation to obesity-related phenotypes. The results show that biomarkers *Candidatus_Saccharimonas*, *Allobaculum*, and *Lachnospiraceae_NK4A136_group* of CK and KON mice were significantly negatively correlated with adipose tissue weight (Fig. 5A, $P < 0.05$). Five biomarkers of MK mice, *Coriobacteriaceae_UCG_002*, *Colidextribacter*, *Faecalibaculum*, *Blautia*, and *Dubosiella*, were significantly positively correlated with body weight, adipose tissue weight, and average adipocyte area (Fig. 5A, $P < 0.05$). Among them, *Coriobacteriaceae_UCG_002*, *Blautia*, and *Dubosiella* were also significantly positively correlated with serum TC (Fig. 5A, $P < 0.05$). In addition, trehalose 6-phosphate and 7-dehydrocholesterol, which are regulated by gut microbiota, were both significantly negatively correlated with adipose tissue weight and mean adipocyte area (Fig. 5A, $P < 0.05$). Trehalose 6-phosphate was also significantly negatively correlated with all serum lipid parameters (Fig. 5A, $P < 0.05$). Glycocholic acid and ursocholic acid in Secondary bile acid biosynthesis are both widely associated with obesity-related phenotypes. They were significantly positively correlated with all obesity-related phenotypes except serum TG (Fig. 5A, $P < 0.05$).

3.4.4. Konjac can alleviate obesity by affecting gut microbiota and gut metabolites

The results of the aforementioned association analysis between gut microbiota and gut metabolites were summarized and Sankey plots were used to make the results more intuitive. Our study shows that under the influence of KGM in konjac powder, the biomarkers *Candidatus_Saccharimonas*, *Allobaculum*, *Coriobacteriaceae_UCG_002*, *Colidextribacter*, *Faecalibaculum*, *Blautia*, *Dubosiella*, and

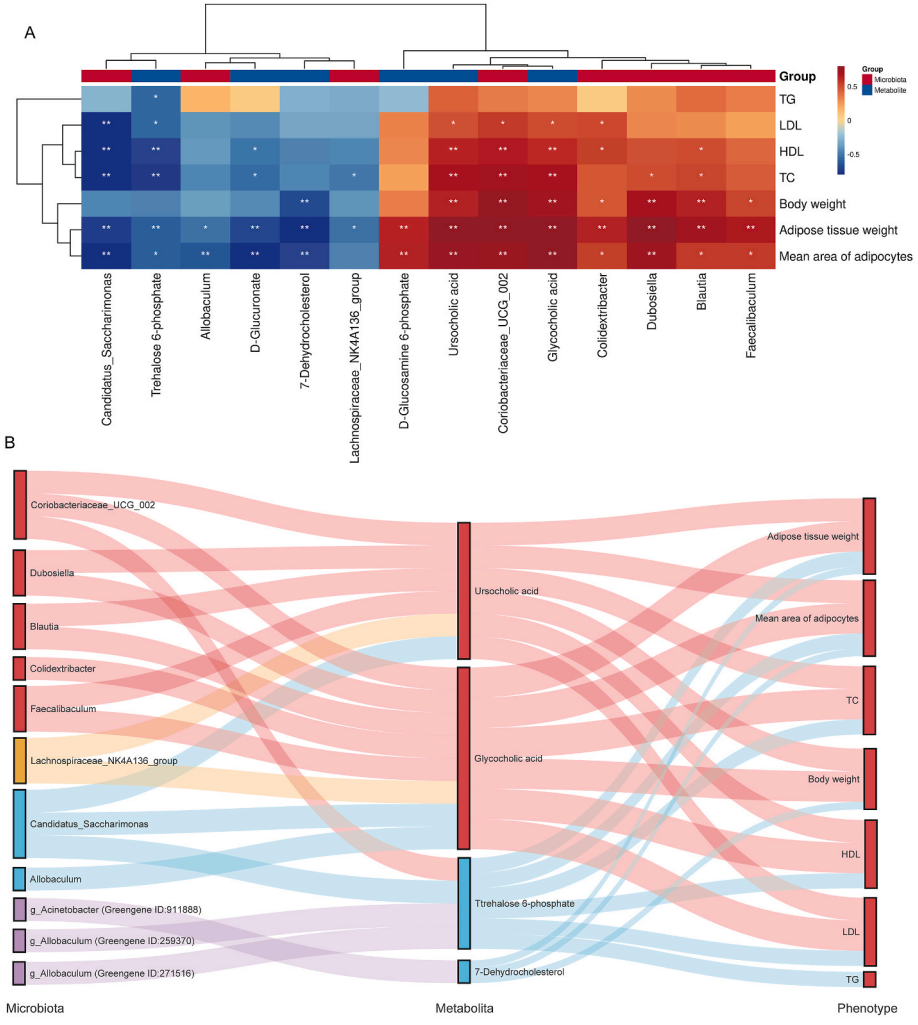

Fig. 5. Correlation analysis and Sankey diagram between gut microbiota, differential metabolites, and obesity-related phenotypes (n = 6 per group). (A) Heat map of correlation analysis between biomarkers from LEfSe analysis, some differential metabolites, and obesity-related phenotypes; and (B) Sankey diagram of gut microbiota-differential metabolism-obesity-related phenotypes. The red nodes in the Sankey diagram represent the biomarkers of MK mice in LEfSe analysis, obesity-related phenotypes and the differential metabolites that are positively correlated with obesity; yellow nodes represent KON mice biomarkers in LEfSe analysis; blue nodes represent CK mice biomarkers in LEfSe analysis and differential metabolites that are negatively correlated with obesity; purple nodes represent key contributors in MIMOSA2 analysis. The red band indicates a positive correlation; yellow and blue bands indicate negative correlations; and purple bands indicate positive contributions. (For interpretation of the references to colour in this figure legend, the reader is referred to the Web version of this article.)

Lachnospiraceae_NK4A136_group, as well as the key contributors in the MIMOSA2 analysis *g_Acinetobacter* (Greengene ID: 911888), *g_Allobaculum* (Greengene ID: 271516), and *g_Allobaculum* (Greengene ID: 259370), could exert anti-obesity effects by improving the levels of glycocholic acid, ursocholic acid, trehalose 6-phosphate, and 7-dehydrocholesterol in the intestine (Fig. 5B).

4. Discussion

Obesity, a multifactorial disease, has emerged as a significant global health concern with a rapidly rising trajectory. Konjac supplementation, a traditional dietary therapy known for its simplicity and efficacy, holds promise as a convenient intervention in the fight against obesity. Our study demonstrates that supplementation with konjac significantly decreased body weight, adipose tissue weight, and serum lipid levels in mice fed a high-fat diet (HFD). This corroborates the results of Kong et al. and Hong et al. (Hong et al., 2023; Kang et al., 2019), but unlike their studies, our study places more emphasis on the therapeutic benefits rather than preventive effects of konjac supplementation on obesity.

The gut microbiota is a significant factor in the pathogenesis of obesity. Research conducted by Jiang et al. demonstrated that oral administration of konjac glucomannan (KGM) enhanced the gut environment and facilitated the growth of beneficial gut bacteria, aligning with our own study findings (Jiang et al., 2018). Our study revealed a notable increase in the relative abundance of *Lachnospiraceae_NK4A136_group*, a biomarker in KON mice, following konjac supplementation. This increase was found to be significantly negatively correlated with a decrease in obesity-related phenotypes. *Lachnospiraceae_NK4A136_group* has been demonstrated to synthesize short-chain fatty acids (SCFAs), such as butyrate, and enhance the integrity of the gut barrier (Ma et al., 2020). Additionally, it activates the PPAR pathway, thereby regulating lipid metabolism, increasing energy expenditure, improving obesity, and reducing body weight (Ai et al., 2022; Zhou et al., 2023). In addition, CK mice biomarkers *Allobaculum* and *Candidatus_Saccharimonas* exhibited significant negative correlations with obesity-related phenotypes. *Allobaculum* demonstrated a beneficial impact on reducing body weight in obese mice and displayed a positive correlation with the expression of ANGPTL4 in the intestine, which can inhibit lipid absorption (Wang et al., 2020; Zheng et al., 2021). Similarly, *Candidatus_Saccharimonas* was found to inhibit obesity and showed negative correlations with serum levels of TG, TC, and free fatty acids (Qi et al., 2024). Furthermore, *Candidatus_Saccharimonas* influenced the occurrence and development of obesity by interacting with COL6A6, a gene involved in inflammation regulation (Qi et al., 2024). In contrast, *Coriobacteriaceae_UCG_002*, *Blautia*, *Faecalibaculum*, and *Dubosiella*, which exhibited significant up-regulation in MK mice, were found to be positively correlated with obesity-related phenotypes. Specifically, *Coriobacteriaceae_UCG_002* demonstrated positive correlations with body weight, serum lipids, and blood glucose in the study conducted by Miao et al. (2023). *Blautia* displayed positive correlations with body weight index, TC, TG, and LDL levels (Zeng et al., 2019). It was observed that reducing the abundance of *Blautia* could potentially alleviate obesity, decrease lipid levels, and regulate glucose homeostasis (Q. Zhao et al., 2022). Research has indicated that the increase of *Faecalibaculum* resulting from a HFD is significantly linked to obesity, subcutaneous fat accumulation, and total cholesterol levels (Cheng et al., 2022). Decreasing *Faecalibaculum* levels could potentially mitigate obesity and dyslipidemia in mice (Cheng et al., 2022). Similarly, the rise in *Dubosiella* is positively correlated with body weight and inversely correlated with SCFAs in fecal matter (Qiu et al., 2021).

The significant role of the interaction between gut microbiota and bile acids in the pathogenesis of obesity is widely recognized, with the farnesoid X receptor (FXR) serving as a key determinant of the impact of gut microbiota and bile acids on the obesity phenotype (Chávez-Talavera et al., 2017; Parséus et al., 2017). Following a HFD, glycocholic acid (GCA) levels were found to be markedly elevated and positively correlated with LDL cholesterol, tumor necrosis factor-α, interleukin (IL)-2, and IL-8 levels (Liang et al., 2020; Osuna-Prieto et al., 2022), aligning with our own research findings. Furthermore, GCA has been found to activate FXR and is modulated by *Bifidobacterium*. Additionally, it is notably linked with *Bacteroidaceae* and *Lachnospiraceae* (Adams et al., 2020; Hibberd et al., 2019; Yao et al., 2024). Similarly to GCA, the elevation of ursocholic acid (UCA) led to the down-regulation of *Bacteroidaceae* and the up-regulation of TC, TG, and LDL (Yan et al., 2023). Despite being an inactive ligand of the FXR and not inducing the FXR receptor-mediated increase in small heterodimer partner (SHP) and bile salt export pump (BSEP) expression, UCA still up-regulated FXR messenger RNA (mRNA) and nuclear protein levels (Li et al., 2005; G. Xu et al., 2002). These findings collectively indicate that both GCA and UCA act as inducers of obesity and can interact with the gut microbiota. The study by Xu et al. also demonstrated that Konjac glucomannan supplementation significantly reduced the content of secondary bile acids in the colon (Y. Xu et al., 2024). In our study, supplementation with konjac was found to significantly modulate secondary bile acid biosynthesis and reverse the upregulation of GCA and UCA induced by a high-fat diet. Additionally, a negative correlation was observed between GCA and UCA levels and biomarkers in CK and KON mice, while a positive correlation was found with the biomarkers in MK mice. These findings suggest that down-regulation of GCA and UCA levels by gut microbiota may be a key mechanism by which Konjac alleviates obesity.

Trehalose, a non-reducing disaccharide, has been shown to enhance energy metabolism and improve lipid levels in obese mouse models through the activation of autophagy (Zhang and DeBosch, 2019). Trehalose 6-phosphate, a precursor in trehalose biosynthesis, demonstrates potent anti-diabetic effects in mammals by enhancing superoxide dismutase activity in islet B cells (Oke and Watt, 1998). Furthermore, the bioactive properties of trehalose are notably influenced by the presence of trehalase, while trehalose 6-phosphate has the ability to suppress trehalose activity, consequently diminishing the degradation of trehalose (Oke and Watt, 1998; Zeng et al., 2019; Zhang et al., 2020). In our study, both trehalose 6-phosphate and trehalose exhibited significant upregulation following konjac supplementation. Trehalose 6-phosphate demonstrated a negative correlation with multiple obesity-related phenotypes and the MK mice biomarker *Coriobacteriaceae_UCG_002*, while displaying a positive correlation with the CK mice biomarker *Candidatus_Saccharimonas*. In addition, MIMOSA2 analysis revealed that *g_Allobaculum* (Greengene ID: 271516) and *g_Allobaculum* (Greengene ID: 259370) could mediate the decomposition of trehalose 6-phosphate by synthesizing glvA, and both contributed positively to the change in the level of trehalose 6-phosphate. These findings suggest that KGM in konjac powder may play a role in reducing obesity by increasing the abundance of trehalose 6-phosphate and trehalose, while trehalose 6-phosphate levels are affected by *g_Allobaculum* (Greengene ID: 271516) and *g_Allobaculum* (Greengene ID: 259370).

7-Dehydrocholesterol (7-DHC), a precursor of Vitamin D3, has been demonstrated to enhance the content of Vitamin D3 in the liver and kidney in a manner dependent on dosage (Kühn et al., 2016). Supplementation with Vitamin D3 has been shown to mitigate weight gain and lower levels of serum cholesterol, LDL, and HDL in obese mice (Zhao and Qin, 2022). Moreover, Vitamin D3 supplementation activates adipocyte autophagy, triggers p53 activation, and inhibits PI3K/Akt/mTOR signaling, thereby playing a crucial role in inducing browning of white adipose tissue and addressing metabolic syndrome, particularly obesity (Y. Zhao et al., 2022). In our study, it was observed that the levels of 7-DHC were significantly reduced following a HFD and exhibited a significant negative correlation with body weight and adipose tissue weight. Conversely, supplementation with konjac led to a significant increase in 7-DHC levels. These findings indicate that konjac supplementation may potentially offer therapeutic benefits for obesity by up-regulating 7-DHC. In addition, MIMOSA2 analysis shows that *g_Acinetobacter* (Greengene ID: 911888) could synthesize ERG3 to promote the synthesis of 7-DHC and positively contribute to 7-DHC alteration.

These findings suggest that *g_Acinetobacter* (Greengene ID: 911888) synthesize ERG3 to upregulate 7-DHC levels, which plays an important role in the potential mechanism of KGM in konjac powder to alleviate obesity.

In this study, KGM in konjac powder was used to treat obesity induced by high-fat diet in mice. 16S rDNA sequencing and untargeted metabolomics were used to explore the effects of KGM in konjac powder on gut microbiota and gut metabolites in obese mice. In the association analysis, in order to explore the potential mechanism of KGM in alleviating obesity through gut microbiota and gut metabolites more broadly, the selected gut bacteria and differential metabolites were directly correlated. But, we screened only the most strongly correlated biomarkers and metabolites and performed a MIMOSA2 analysis, which can also give considerable strength to our conclusions. However, this study also has some limitations. For example, we did not further validate gut bacteria or gut metabolites that may play key roles in the association analysis, which limits the certainty of our conclusions. In addition, we did not supplement konjac powder to mice on a low-fat diet. The role of KGM in alleviating obesity may be more fully explored if mice fed on a low-fat diet or a normal diet were supplemented with konjac powder.

5. Conclusion

Our study confirmed that KGM in konjac powder can reduce the body weight, adipose tissue weight, and serum lipid level of high-fat diet induced obese mice. Association analysis revealed that KGM supplementation induced changes in gut microbiota, resulting in the up-regulation of 7-dehydrocholesterol and trehalose 6-phosphate, as well as the down-regulation of glycocholic acid and ursocholic acid, ultimately leading to improvements in obesity. Among them, *g_Acinetobacter* (Greengene ID: 911888) can promote the synthesis of 7-dehydrocholesterol, *g_Allobaculum* (Greengene ID: 271516) and *g_Allobaculum* (Greengene ID: 259370) can promote the breakdown of trehalose 6-phosphate. Additionally, the down-regulation of glycocholic acid and ursocholic acid may be influenced by the up-regulation of *Lachnospiraceae_NK4A136_group*. In conclusion, KGM exerts an influence on gut metabolites through the regulation of gut microbiota, thereby playing a pivotal role in alleviating obesity induced by a high-fat diet.

Funding

This work was supported by PhD Start-up funding of Southwest Medical University (grant number: 66/00170054).

CRediT authorship contribution statement

Yuhang Wen: Conceptualization, Data curation, Formal analysis, Investigation, Methodology, Validation, Visualization, Writing – original draft, Writing – review & editing. **Baoting Chen:** Data curation, Investigation, Writing – original draft. **Jingrong Huang:** Data curation, Investigation, Validation, Writing – original draft. **Yadan Luo:** Data curation, Formal analysis, Methodology, Visualization, Writing – original draft, Writing – review & editing. **Shuya Lv:** Data curation, Visualization, Writing – review & editing. **Hao Qiu:** Conceptualization, Data curation, Investigation, Writing – review & editing. **Shuaibing Li:** Data curation, Investigation, Writing – review & editing. **Songwei Liu:** Data curation, Investigation. **Lvqin He:** Data curation, Writing – review & editing. **Manli He:** Funding acquisition, Project administration, Supervision, Validation, Writing – review & editing. **Zehui Yu:** Data curation, Writing – review & editing. **Mingde Zhao:** Data curation, Writing – review & editing. **Qian Yang:** Conceptualization, Writing – review & editing. **Dong Li:** Funding acquisition, Project administration, Supervision, Writing – review & editing. **Congwei Gu:** Conceptualization, Formal analysis, Funding acquisition, Project administration, Supervision, Writing – review & editing.

Declaration of competing interest

The authors declare that the research was conducted in the absence of any commercial or financial relationships that could be construed as a potential conflict of interest.

Data availability

I have shared the link to my data in the manuscript

Acknowledgements

We thank the Laboratory Animal Center of Southwest Medical University for technical support and the PhD Start-up funding of Southwest Medical University (66/00170054).

Appendix A. Supplementary data

Supplementary data to this article can be found online at https://doi.org/10.1016/j.crfs.2024.100805.

References

Adams, L.A., Wang, Z., Liddle, C., Melton, P.E., Ariff, A., Chandraratna, H., Jeffrey, G.P., 2020. Bile acids associate with specific gut microbiota, low-level alcohol consumption and liver fibrosis in patients with non-alcoholic fatty liver disease. Liver Int. 40 (6), 1356–1365. https://doi.org/10.1111/liv.14453.

Ai, Z.L., Zhang, X., Ge, W., Zhong, Y.B., Wang, H.Y., Zuo, Z.Y., Liu, D.Y., 2022. Salvia miltiorrhiza extract may exert an anti-obesity effect in rats with high-fat diet-induced obesity by modulating gut microbiome and lipid metabolism. World J. Gastroenterol. 28 (43), 6131–6156. https://doi.org/10.3748/wjg.v28.i43.6131.

Aron-Wisnewsky, J., Clément, K., Nieuwdorp, M., 2019. Fecal microbiota transplantation: a future therapeutic option for obesity/diabetes? Curr. Diabetes Rep. 19 (8), 51. https://doi.org/10.1007/s11892-019-1180-z.

Boulangé, C.L., Neves, A.L., Chilloux, J., Nicholson, J.K., Dumas, M.E., 2016. Impact of the gut microbiota on inflammation, obesity, and metabolic disease. Genome Med. 8 (1), 42. https://doi.org/10.1186/s13073-016-0303-2.

Breit, S.N., Brown, D.A., Tsai, V.W.W., 2023. GDF15 analogs as obesity therapeutics. Cell Metabol. 35 (2), 227–228. https://doi.org/10.1016/j.cmet.2023.01.002.

Caballero, B., 2019. Humans against obesity: who will win? Adv. Nutr. 10 (Suppl. l_1), S4–s9. https://doi.org/10.1093/advances/nmy055.

Cani, P.D., Possemiers, S., Van de Wiele, T., Guiot, Y., Everard, A., Rottier, O., Delzenne, N.M., 2009. Changes in gut microbiota control inflammation in obese mice through a mechanism involving GLP-2-driven improvement of gut permeability. Gut 58 (8), 1091–1103. https://doi.org/10.1136/gut.2008.165886.

Caruso, A., Gelsomino, L., Panza, S., Accattatis, F.M., Naimo, G.D., Barone, I., Andò, S., 2023. Leptin: a heavyweight player in obesity-related cancers. Biomolecules 13 (7). https://doi.org/10.3390/biom13071084.

Chandrasekaran, P., Weiskirchen, R., 2024. The role of obesity in type 2 diabetes mellitus-an overview. Int. J. Mol. Sci. 25 (3) https://doi.org/10.3390/ijms25031882.

Chávez-Talavera, O., Tailleux, A., Lefebvre, P., Staels, B., 2017. Bile acid control of metabolism and inflammation in obesity, type 2 diabetes, dyslipidemia, and nonalcoholic fatty liver disease. Gastroenterology 152 (7), 1679–1694.e1673. https://doi.org/10.1053/j.gastro.2017.01.055.

Cheng, L., Wei, Y., Xu, L., Peng, L., Wang, Y., Wei, X., 2022. Gut microbiota differentially mediated by qingmao tea and qingzhuan tea alleviated high-fat-induced obesity and associated metabolic disorders: the impact of microbial fermentation. Foods 11 (20). https://doi.org/10.3390/foods11203210.

Cuevas-Sierra, A., Ramos-Lopez, O., Riezu-Boj, J.I., Milagro, F.I., Martinez, J.A., 2019. Diet, gut microbiota, and obesity: links with host genetics and epigenetics and potential applications. Adv. Nutr. 10 (Suppl. l_1), S17–s30. https://doi.org/10.1093/advances/nmy078.

Dong Li, W.T., Jiang, Bin, Wang, Yangli, Li, Rui, Lei, Yu, Tong, Kai, Kang, Zhenhui, Yan, Liping, Li, Yalan, Tang, Xuan, Li, Jieyuan, 2020. Study on production technology and character analysis of konjac powder by ball milling method. China Condimen 45 (7), 23–27. https://doi.org/10.3969/j.issn.1000-9973.2020.07.006.

Hibberd, A.A., Yde, C.C., Ziegler, M.L., Honoré, A.H., Saarinen, M.T., Lahtinen, S., Stenman, L.K., 2019. Probiotic or synbiotic alters the gut microbiota and metabolism in a randomised controlled trial of weight management in overweight adults. Benef. Microbes 10 (2), 121–135. https://doi.org/10.3920/bm2018.0028.

Ho, H.V.T., Jovanovski, E., Zurbau, A., Blanco Mejia, S., Sievenpiper, J.L., Au-Yeung, F., Vuksan, V., 2017. A systematic review and meta-analysis of randomized controlled trials of the effect of konjac glucomannan, a viscous soluble fiber, on LDL cholesterol and the new lipid targets non-HDL cholesterol and apolipoprotein B. Am. J. Clin. Nutr. 105 (5), 1239–1247. https://doi.org/10.3945/ajcn.116.142158.

Hong, J., Shi, Y., Chen, J., Mi, M., Ren, Q., Zhang, Y., Kang, Y., 2023. Konjac glucomannan attenuate high-fat diet-fed obesity through enhancing β-adrenergic-

mediated thermogenesis in inguinal white adipose tissue in mice. Glycoconj. J. 40 (5), 575–586. https://doi.org/10.1007/s10719-023-10131-w.
Jian, W., Tu, L., Wu, L., Xiong, H., Pang, J., Sun, Y.M., 2017. Physicochemical properties and cellular protection against oxidation of degraded Konjac glucomannan prepared by γ-irradiation. Food Chem. 231, 42–50. https://doi.org/10.1016/j.foodchem.2017.03.121.
Jiang, M., Li, H., Shi, J.S., Xu, Z.H., 2018. Depolymerized konjac glucomannan: preparation and application in health care. J. Zhejiang Univ. - Sci. B 19 (7), 505–514. https://doi.org/10.1631/jzus.B1700310.
Kang, Y., Li, Y., Du, Y., Guo, L., Chen, M., Huang, X., Kong, X., 2019. Konjaku flour reduces obesity in mice by modulating the composition of the gut microbiota. Int. J. Obes. 43 (8), 1631–1643. https://doi.org/10.1038/s41366-018-0187-x.
Kühn, J., Hirche, F., Geissler, S., Stangl, G.I., 2016. Oral intake of 7-dehydrocholesterol increases vitamin D(3) concentrations in the liver and kidney. J. Steroid Biochem. Mol. Biol. 164, 199–204. https://doi.org/10.1016/j.jsbmb.2015.12.017.
Li, H., Chen, F., Shang, Q., Pan, L., Shneider, B.L., Chiang, J.Y., Xu, G., 2005. FXR-activating ligands inhibit rabbit ASBT expression via FXR-SHP-FTF cascade. Am. J. Physiol. Gastrointest. Liver Physiol. 288 (1), G60–G66. https://doi.org/10.1152/ajpgi.00170.2004.
Liang, L.M., Zhou, J.J., Xu, F., Liu, P.H., Qin, L., Liu, L., Liu, X.D., 2020. Diabetes downregulates peptide transporter 1 in the rat jejunum: possible involvement of cholate-induced FXR activation. Acta Pharmacol. Sin. 41 (11), 1465–1475. https://doi.org/10.1038/s41401-020-0408-4.
Liu, Q., Fang, J., Huang, W., Liu, S., Zhang, X., Gong, G., Wang, Z., 2023. The intervention effects of konjac glucomannan with different molecular weights on high-fat and high-fructose diet-fed obese mice based on the regulation of gut microbiota. Food Res. Int. 165, 112498 https://doi.org/10.1016/j.foodres.2023.112498.
Ma, L., Ni, Y., Wang, Z., Tu, W., Ni, L., Zhuge, F., Fu, Z., 2020. Spermidine improves gut barrier integrity and gut microbiota function in diet-induced obese mice. Gut Microb. 12 (1), 1–19. https://doi.org/10.1080/19490976.2020.1832857.
Marcelin, G., Silveira, A.L.M., Martins, L.B., Ferreira, A.V., Clément, K., 2019. Deciphering the cellular interplays underlying obesity-induced adipose tissue fibrosis. J. Clin. Invest. 129 (10), 4032–4040. https://doi.org/10.1172/jci129192.
Marchesi, J.R., Adams, D.H., Fava, F., Hermes, G.D., Hirschfield, G.M., Hold, G., Hart, A., 2016. The gut microbiota and host health: a new clinical frontier. Gut 65 (2), 330–339. https://doi.org/10.1136/gutjnl-2015-309990.
Miao, Z., Zheng, H., Liu, W.H., Cheng, R., Lan, H., Sun, T., He, F., 2023. Lacticaseibacillus paracasei K56 attenuates high-fat diet-induced obesity by modulating the gut microbiota in mice. Probiotics Antimicrob Proteins 15 (4), 844–855. https://doi.org/10.1007/s12602-022-09911-x.
Noecker, C., Eng, A., Muller, E., Borenstein, E., 2022. MIMOSA2: a metabolic network-based tool for inferring mechanism-supported relationships in microbiome-metabolome data. Bioinformatics 38 (6), 1615–1623. https://doi.org/10.1093/bioinformatics/btac003.
Oke, J.M., Watt, R.A., 1998. Hypoglycaemic activity of alpha, alpha trehalose-6-phosphate. Afr. J. Med. Med. Sci. 27 (3–4), 219–223.
Osuna-Prieto, F.J., Rubio-Lopez, J., Di, X., Yang, W., Kohler, I., Rensen, P.C.N., Martinez-Tellez, B., 2022. Plasma levels of bile acids are related to cardiometabolic risk factors in young adults. J. Clin. Endocrinol. Metab. 107 (3), 715–723. https://doi.org/10.1210/clinem/dgab773.
Parséus, A., Sommer, N., Sommer, F., Caesar, R., Molinaro, A., Ståhlman, M., Bäckhed, F., 2017. Microbiota-induced obesity requires farnesoid X receptor. Gut 66 (3), 429–437. https://doi.org/10.1136/gutjnl-2015-310283.
Qi, W., Zhu, S., Feng, L., Liang, J., Guo, X., Cheng, F., Liang, J., 2024. Integrated analysis of the transcriptome and microbial diversity in the intestine of miniature pig obesity model. Microorganisms 12 (2). https://doi.org/10.3390/microorganisms12020369.
Qiu, X., Macchietto, M.G., Liu, X., Lu, Y., Ma, Y., Guo, H., Chen, X., 2021. Identification of gut microbiota and microbial metabolites regulated by an antimicrobial peptide lipocalin 2 in high fat diet-induced obesity. Int. J. Obes. 45 (1), 143–154. https://doi.org/10.1038/s41366-020-00712-2.
Rogovik, A.L., Goldman, R.D., 2009. Should weight-loss supplements be used for pediatric obesity? Can. Fam. Physician 55 (3), 257–259.
Tester, R.F., Al-Ghazzewi, F.H., 2016. Beneficial health characteristics of native and hydrolysed konjac (Amorphophallus konjac) glucomannan. J. Sci. Food Agric. 96 (10), 3283–3291. https://doi.org/10.1002/jsfa.7571.
Wang, Y., Tang, C., Tang, Y., Yin, H., Liu, X., 2020. Capsaicin has an anti-obesity effect through alterations in gut microbiota populations and short-chain fatty acid concentrations. Food Nutr. Res. 64 https://doi.org/10.29219/fnr.v64.3525.
Xu, C., Yu, C., Yang, S., Deng, L., Zhang, C., Xiang, J., Shang, L., 2023. Effects of physical properties of konjac glucomannan on appetite response of rats. Foods 12 (4). https://doi.org/10.3390/foods12040743.
Xu, G., Pan, L.X., Li, H., Forman, B.M., Erickson, S.K., Shefer, S., Salen, G., 2002. Regulation of the farnesoid X receptor (FXR) by bile acid flux in rabbits. J. Biol. Chem. 277 (52), 50491–50496. https://doi.org/10.1074/jbc.M209176200.
Xu, Y., Zhou, C., Zong, M., Zhu, J., Guo, X., Sun, Z., 2024. High-protein high-konjac glucomannan diets changed glucose and lipid metabolism by modulating colonic microflora and bile acid profiles in healthy mouse models. Food Funct. 15 (8), 4446–4461. https://doi.org/10.1039/d4fo00159a.
Yan, J., Zhang, R., Kang, J., Zhong, Y., Abudurexiti, A., Tan, H., Ma, X., 2023. Effect of Cichorium glandulosum on intestinal microbiota and bile acid metabolism in db/db mice. Food Sci. Nutr. 11 (12), 7765–7778. https://doi.org/10.1002/fsn3.3694.
Yao, S., Ren, S., Cai, C., Cao, X., Shi, Y., Wu, P., Ye, Y., 2024. Glycocholic acid supplementation improved growth performance and alleviated tissue damage in the liver and intestine in Pelteobagrus fulvidraco fed a high-pectin diet. Fish Physiol. Biochem. 50 (1), 41–57. https://doi.org/10.1007/s10695-022-01148-3.
Zeng, Q., Li, D., He, Y., Li, Y., Yang, Z., Zhao, X., Dai, W., 2019. Discrepant gut microbiota markers for the classification of obesity-related metabolic abnormalities. Sci. Rep. 9 (1), 13424 https://doi.org/10.1038/s41598-019-49462-w.
Zhang, Y., DeBosch, B.J., 2019. Using trehalose to prevent and treat metabolic function: effectiveness and mechanisms. Curr. Opin. Clin. Nutr. Metab. Care 22 (4), 303–310. https://doi.org/10.1097/mco.0000000000000568.
Zhang, Y., Shaikh, N., Ferey, J.L., Wankhade, U.D., Chintapalli, S.V., Higgins, C.B., DeBosch, B.J., 2020. Lactotrehalose, an analog of trehalose, increases energy metabolism without promoting clostridioides difficile infection in mice. Gastroenterology 158 (5), 1402–1416.e1402. https://doi.org/10.1053/j.gastro.2019.11.295.
Zhao, Q., Fu, Y., Zhang, F., Wang, C., Yang, X., Bai, S., Shen, Q., 2022. Heat-treated adzuki bean protein hydrolysates reduce obesity in mice fed a high-fat diet via remodeling gut microbiota and improving metabolic function. Mol. Nutr. Food Res. 66 (8), e2100907 https://doi.org/10.1002/mnfr.202100907.
Zhao, Y., Jayachandran, M., Xu, B., 2020. In vivo antioxidant and anti-inflammatory effects of soluble dietary fiber Konjac glucomannan in type-2 diabetic rats. Int. J. Biol. Macromol. 159, 1186–1196. https://doi.org/10.1016/j.ijbiomac.2020.05.105.
Zhao, Y., Qin, R., 2022. Vitamin D3 affects browning of white adipocytes by regulating autophagy via PI3K/Akt/mTOR/p53 signaling in vitro and in vivo. Apoptosis 27 (11–12), 992–1003. https://doi.org/10.1007/s10495-022-01765-6.
Zheng, Z., Lyu, W., Ren, Y., Li, X., Zhao, S., Yang, H., Xiao, Y., 2021. Allobaculum involves in the modulation of intestinal ANGPTLT4 expression in mice treated by high-fat diet. Front. Nutr. 8, 690138 https://doi.org/10.3389/fnut.2021.690138.
Zhou, X., Pak, S., Li, D., Dong, L., Chen, F., Hu, X., Ma, L., 2023. Bamboo shoots modulate gut microbiota, eliminate obesity in high-fat-diet-fed mice and improve lipid metabolism. Foods 12 (7). https://doi.org/10.3390/foods12071380.